An Intracavity Laser Temperature Jump Apparatus and Its Application to the Interaction of Methylisonitrile with Hemoglobin β Chains

John H. Baldo,[1] Barbara A. Manuck,[1] E. B. Priestley,[2] and Brian D. Sykes*[1,3]

Contribution from the Department of Chemistry and the Division of Engineering and Applied Physics, Harvard University, Cambridge, Massachusetts 02138. *Received September 5, 1974*

Abstract: A laser temperature jump apparatus has been constructed which produces large temperature rises and uniform sample heating by placing the sample within the laser cavity. This intracavity design achieves substantial, direct absorption of the 1.06 μ laser radiation by multiple passes of the laser radiation through the sample. The construction is very simple and the operation sufficiently stable so that signal averaging of transients is routine. This apparatus has been used to study the interaction of hemoglobin β chains with methylisonitrile and the results are compared with the rate constants obtained with nuclear magnetic resonance methods under similar sample conditions.

A laser heated temperature jump apparatus offers several advantages over the conventional joule heating apparatus.[4-8] The most obvious is the possibility for studying very fast reactions, due to the rapid heating times (~10 nsec) achievable using Q-switched laser pulses. The second is the greater freedom in designing the sample cell which results from the elimination of the two large electrodes in contact with the solution required in the joule heating experiment. The third is the removal of any constraint upon the conductance of the sample, with the concomitant possibility of using nonaqueous solvents. A mixed blessing results from the fact that the intense laser light can also cause photochemical reaction in some solutions.[9-11]

The simplest and best means of achieving laser heating of a solution is via the direct absorption of the laser radiation by the solvent. However, the absorption bands of most of the frequently used solvents are not coincident with the output frequencies of conveniently available high power lasers; in the case of H_2O, for example, the absorption coefficient is negligibly small at 0.694 μm (ruby) and only 0.067 cm^{-1} at 1.06 μm (neodymium). The two approaches which have been used most often in circumventing this difficulty are (i) to Raman shift the laser frequency to a wavelength where the solvent absorbs more strongly[6,11,12] or, alternatively, (ii) to introduce dyes into the solution which absorb at the laser frequency and which subsequently transfer their excitation energy to the solvent.[5,7,13-18] Neither of these approaches is completely satisfactory. While the Raman shifting technique permits additional flexibility in matching excitation frequencies with absorption bands, it is still limited. Too strong an absorption is as undesirable as too weak an absorption, since longitudinal thermal gradients in the sample become very large. Clearly it is not always easy to achieve the optimal absorption strength by the Raman shifting technique. On the other hand, the addition of a dye to the solution is often undesirable and the characteristics of the dye (bleaching, lifetime of excited states, etc.) are critical.

We are interested in using laser temperature jump methods to study biochemical reactions. Because of the advantages cited earlier, many biochemical systems that are either unstable under high salt aqueous solution conditions or are incompatible with high current (e.g., redox reactions), both of which are present in conventional joule heating experiments, are opened for study. The laser temperature jump apparatus which we have constructed permits substantial, direct absorption of 1.06 μm laser radiation by the weak, 1 μm solvent (water) bands by putting the sample cell inside the laser cavity and thereby achieving multiple passes of the laser radiation through the sample. This avoids both the addition of dyes which can bind to biomacromolecules and nonlinear heating problems associated with high absorbances. The apparatus is sufficiently stable that signal averaging of weak transients is routine. We have used this system to study the binding of methylisonitrile to hemoglobin β chains, and present a comparison of the rate constants obtained with those determined for the same reaction using nuclear magnetic resonance techniques.[19]

Experimental Section

(A) Apparatus.[20] Figure 1A is a block diagram of the complete system. A Nova 1220 computer performs both experimental control and data acquisition functions. The computer can be accessed either by means of a teletype terminal or a magnetic tape drive (Computer Operations, Inc.). A Biomation 610B transient recorder serves both as an analog-to-digital converter and as a data buffer. Continuous display of the most recent transient and the current accumulated transient is provided by an oscilloscope through a Megatek oscilloscope interface connected to the computer. This permits visual examination of individual transients by the operator before they are added to the accumulated data in the memory. The final, averaged transient is stored on magnetic tape for later analysis by nonlinear least-squares methods. Hard copy plots of the data can also be obtained on an X-Y recorder.

Details of the experimental apparatus are shown in Figure 1B. The laser cavity is formed by mirrors M_1 and M_2 which are separated by approximately 1 m. A Space Rays laser head (Model No. 1010-C2) equipped with a $\frac{5}{8}$ in. × 7 in. neodymium-doped glass rod is situated near one of the mirrors, M_1; the sample cell is located near M_2, *inside* the plane parallel cavity. When operated normal mode, the laser has a rated maximum output of 60 J and a pulse width of ~0.2 msec (see Figure 2). A Corning glass infrared pass filter F (C.S. 2-64) prevents visible flashlamp light from reaching the optical detection system. Lens L_1 focuses the beam so that its cross-section at the sample cell represents a reasonable compromise in achieving the benefits of increased energy density (due to focusing) while maintaining minimum transverse temperature gradients (arising from the nonsquare intensity profile of the beam). In practice, the beam cross-section at the sample is roughly three times the area of the active sample.

The optical detection system consists of an Electro Powerpacks power supply and lamp housing (Electro Powerpacks 371, 354, 359) fitted with a tungsten-halogen lamp, a Bausch & Lomb high intensity monochromator (No. 33-86-07) with visible grating (350-800 nm), the sample cell and housing, and an RCA 1P28 photomultiplier. Lenses L_2 and L_3 serve to collect and focus light from the tungsten-halogen lamp on the entrance slit of the monochromator. The monochromator has a reciprocal linear dispersion of 7.4 μm/mm and was used with entrance and exit slit widths of the order of 1-3 mm.

The sample cells, made of grade A1 optical quartz by Pyrocell, Inc., hold 30 μl of liquid (ca. 0.3 × 0.3 × 0.3 mm^3) and were specially constructed so they can be sealed to exclude atmospheric

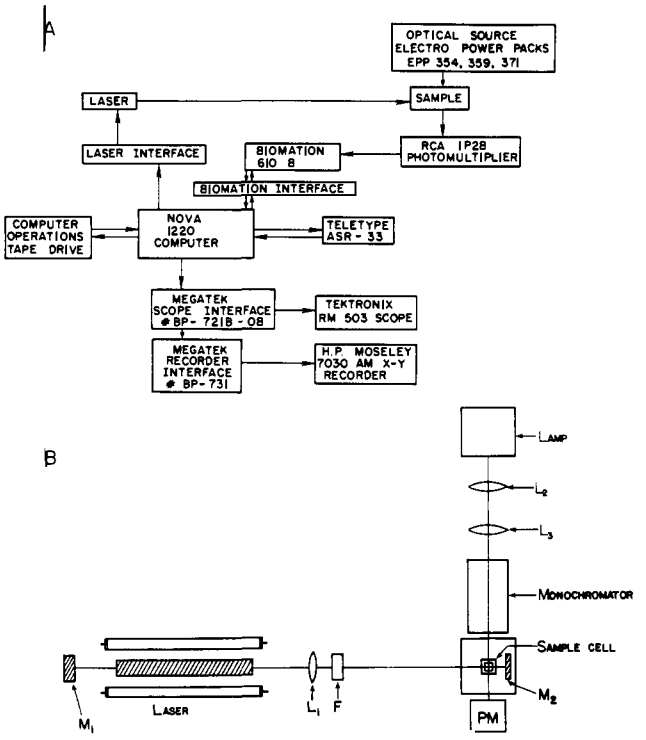

Figure 1. (A) Simplified block diagram of laser T jump apparatus. (B) Schematic layout of the optical components of the laser T jump apparatus: M, mirror; L, lens; F, filter; P.M. photomultiplier tube.

gases but still allow for expansion in the upper part of the cell.

Temperature calibrations were made using a 0.1 M Tris–Phenol Red solution with an absorbance of 0.74 and pH of 8.1 at 25°. Calibration of the absorbance change of the dye solution as a function of temperature, using a Gilford spectrophotometer and a Lauda constant temperature bath, gave approximately 104° per unit change in absorbance.

(B) Materials. The samples containing hemoglobin β chains (β^{PMB}) and methylisonitrile (MIN) were prepared by placing $\simeq$5 mg of sodium dithionite in the bottom of a serum-capped temperature jump cell, which was then flushed with argon (see ref 19 for details of the preparation of β^{PMB} and MIN). Potassium phosphate buffer (0.2 M, pH 7) was then injected with a syringe, and deoxygenated by bubbling argon through the solution for 0.5 hr. Finally the required small volumes of stock β^{PMB} ($\approx$0.3 mM) and MIN ($\sim$0.001 M) solutions were added to the buffer. Optical spectra were taken for each sample before and after the addition of MIN. One spectrum (650–500 nm) was taken immediately after the addition of β^{PMB} to determine the initial concentration of deoxy β^{PMB} chains. A final spectrum was taken after the addition of MIN to determine the fractional saturation of β^{PMB} with MIN.

Results

(A) Operation of the Laser Temperature Jump System. Simple interpretation of the results of any temperature jump experiment requires uniform heating of the entire sample on a time scale fast compared to the reaction rates of interest. One of the principal advantages of a laser heated temperature jump apparatus is the *rapid* heating achievable using Q-switched laser pulses. However, achieving *uniform* heating is a much more difficult task, due to the Beer's law exponential absorption from front to back of the sample. All of the laser heated temperature jump experiments reported in the literature[5-7,11-18] have suffered to a greater or lesser extent from nonuniform longitudinal temperature profiles. It is in the alleviation of precisely this difficulty that we feel the present intracavity scheme has the most to offer. Because of the multipass nature of the intracavity configuration, one can utilize a weak absorption band, for which the exponential factor changes only slightly

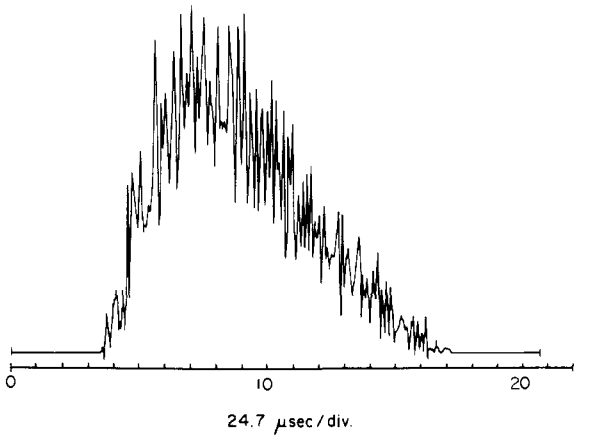

Figure 2. Trace of the laser pulse. The pulse was detected by an EG+G YAG-100 silicon photodiode and after amplification, the signal was processed in the same manner as T jump transients. The trace is the sum of eight pulses, each collected at a rate of one point every 2 μsec for 256 points. Horizontal scale: 24.7 μsec/division.

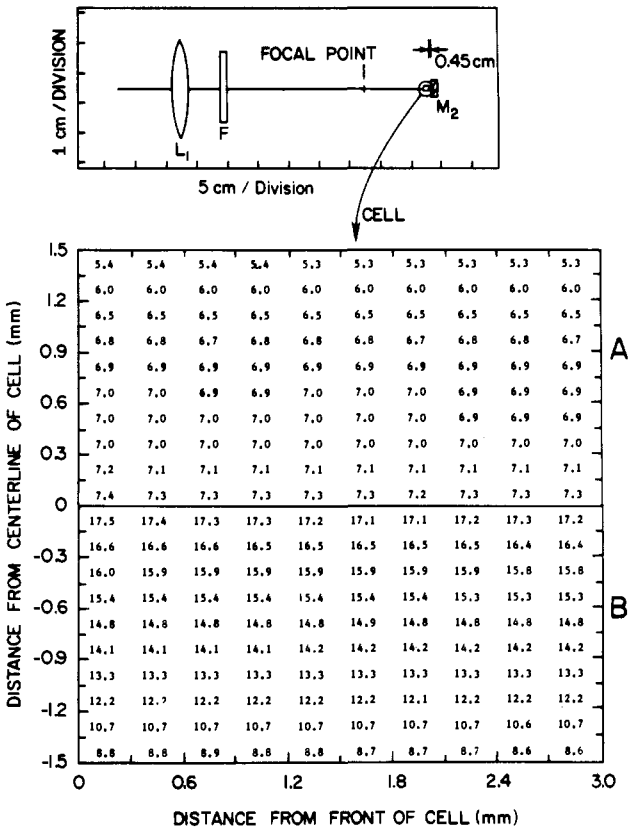

Figure 3. A plot of the calculated temperature contour of the cell: (A) for the configuration shown in Figure 1B; (B) with filter removed. Alternate halves of the cell are shown for the two simulations.

over the thickness of the sample, and still produce substantial temperature rises (>10°).

A computer simulation of the intracavity system was carried out to determine the temperature distribution within the cell. The distances between the optical elements and the apertures of the optical elements are presented in Figure 3. The loss on dielectric coated surfaces was taken to be 0.2% (nominal manufacturer's specifications) and the loss on uncoated surfaces was taken to be 4%. The transmission of the Corning filter at 1.06 μ is 84%. The absorbance of water was taken to be 0.067 cm^{-1}.[6,15] A bundle of initially parallel, evenly spaced, and isoenergetic rays (see Discussion section) was then started out in the laser rod and passed through the system from mirror to mirror. The total initial

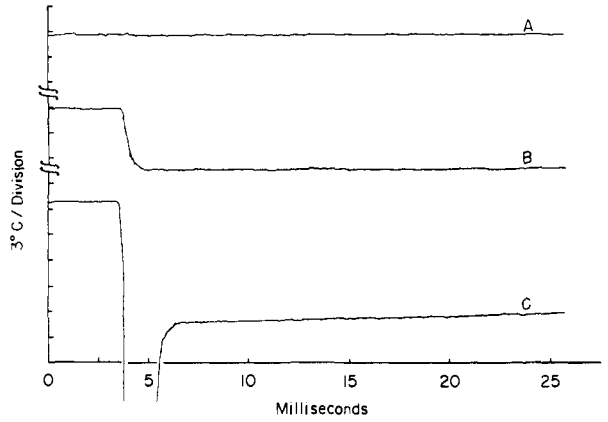

Figure 4. Heating pulse profile using 0.1 *M* Tris–HCl and Phenol Red, pH 8.1, optical density 0.77 at 21°. Trace A is the background in the absence of a laser pulse, i.e., with mirror M_2 removed; trace B is the heating profile obtained using the configuration shown in Figure 1B; trace C is without the filter. The horizontal sampling rate was 0.1 msec per point for 256 points corresponding to 1.25 msec/division; vertical scale 3°/division. All traces are sums of four individual traces.

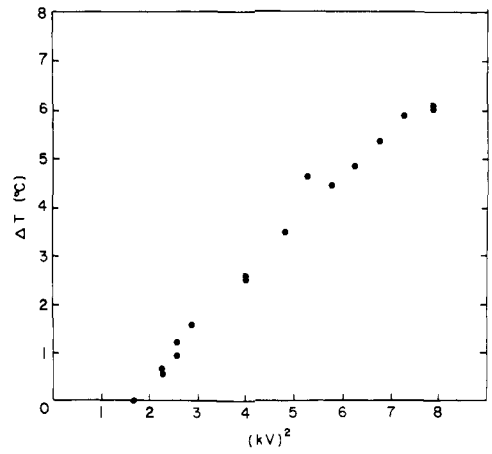

Figure 5. Plot of temperature jump as a function of charge on the laser storage capacitors with laser configuration as shown in Figure 1B with optical flat added. The temperature jump was measured by using a solution of Phenol Red in 0.1 *M* Tris–HCl, pH 8.1; OD is 0.9 at 29° and 560 mμ.

energy in the bundle of rays was taken to correspond to the specific experimental conditions simulated. For a constant cavity configuration, the only variable was the electrical energy discharged through the flashlamps. Thus for a charge voltage of 2.4 kV, at which most experiments were performed, the total initial energy was calculated to be 4.08 calories based upon experimental results (see below, Figure 5) which show that no temperature rise is obtained at a charge voltage of 1.3 kV and the rated output of the laser (14.35 calories) at the maximum charge voltage of 4 kV.[21] At each optical element every ray was tested to determine whether it passed through the element and then its energy was attenuated by the appropriate amount. All rays that did not pass through the element were discarded. The sample cell was divided up into a grid so that any ray passing through a unit in the grid could be attenuated by an appropriate amount and that energy added to the sum of energy already in the unit. The energy sum in each unit of the grid was then converted to a temperature rise.

The changes in temperature can then be plotted as a function of position in the grid to form a temperature contour. The contour for the experimental set-up shown in Figure 1B is given in Figure 3A. The average calculated temperature rise over the grid was 6.7°. In a similar manner it was possible to add an optical flat (see below) to the simulation. In this case the calculated average temperature rise was 5.7° and the transverse heating profile was flatter. Correspondingly, when the filter was removed from the simulation the calculated average temperature rise was 13.9°. However, the transverse heating profile became more domed shaped (Figure 3B). When the charge on the power capacitors was reduced to 1.7 kV for the latter configuration, the calculated average temperature rise dropped to 4.1°.

The observed sample heating curves are shown in Figure 4. Trace A shows the background in the absence of a laser pulse, i.e., with mirror M_2 removed. Trace B shows the temperature rise (7.2°) when the system is operated as shown in Figure 1B. Each division on the vertical scale corresponds to 3°. Trace C shows the temperature rise when the filter F is removed from the cavity. Since the filter represents a substantial loss within the cavity, the temperature rise almost doubles, to 13.4°, upon its removal. When the charging voltage was reduced to 1.7 kV, the observed temperature rise in this configuration was 5.1°. However, without the filter, some of the visible flashlamp light reaches the photomultiplier and is seen as an initial spike (See Figure 4C). For this reason, the experimental configuration used included the filter. In addition, an optical flat was placed in the cavity between the laser head and L_1 for alignment purposes. This resulted in a reduction of the temperature rise from 7.2 to 6.0°.

The temperature rise is a function of the electrical energy discharged through the flashlamps, which was 2.4 kV across 750 μF for traces A–C. Since the temperature jump is nearly proportional to the square of the charge voltage and the instrument is designed for 4 kV, correspondingly higher temperature jumps can be achieved. This is seen in Figure 5 for the configuration shown in Figure 1B with the optical flat added.

The observed half-time for the return of the cell to room temperature was 0.9 sec.

The laser pulses have proven to be quite reproducible in time and energy and individual transients can be easily overlaid on each other. This reproducibility has made signal averaging routine. Most of the transient records analyzed below are the average of eight transients.

(B) Application to the Interaction of Hemoglobin β Chains with Methylisonitrile. Averaged transient records after several successive temperature jumps for β^{PMB} chains plus MIN were obtained by following the change in absorbance at 430, 440, 450, and 530 nm. A typical transient record is shown in Figure 6. No transients were observable for either buffer plus MIN alone, or β^{PMB} chains alone. The rate constants obtained were wavelength independent and are presented in Table I along with the initial concentrations of β^{PMB} and MIN. The concentration of free β^{PMB} plus free MIN ($\bar{\beta} + \bar{M}$) determined optically along with the dissociation constant for the interaction, calculated for each set of concentrations from the optical spectrum, are also presented. Since the calculated free concentrations are sensitive to small errors in the optical measurements with these small cells, the rate constants k_{-1} and k_1 were obtained in the following manner. Assuming a simple bimolecular reaction

$$\beta^{PMB} + MIN \underset{k_{-1}}{\overset{k_1}{\rightleftharpoons}} \beta^{PMB}(MIN) \quad (1)$$

the concentration dependence of the inverse of the half-time for the transient is of the following form[22]

$$1/\tau = k_{-1} + k_1(\bar{\beta} + \bar{M}) \quad (2)$$

A plot of $1/\tau$ vs. $(\bar{\beta} + \bar{M})$ calculated from the optical data was then constructed. This plot gave estimates for k_{-1} and

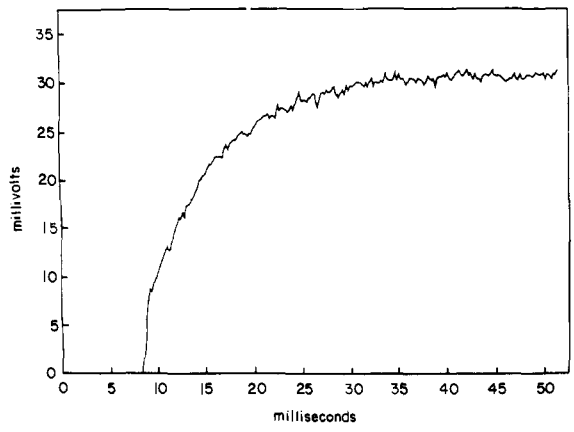

Figure 6. A typical temperature jump transient. Hemoglobin β chain + methylisonitrile free = 0.076 mM, τ = 7.7 msec. This trace is the sum of six individual transients. Horizontal scale 2.5 msec/cm, vertical scale 2.5 mV/cm. The temperature jump was 5.7°.

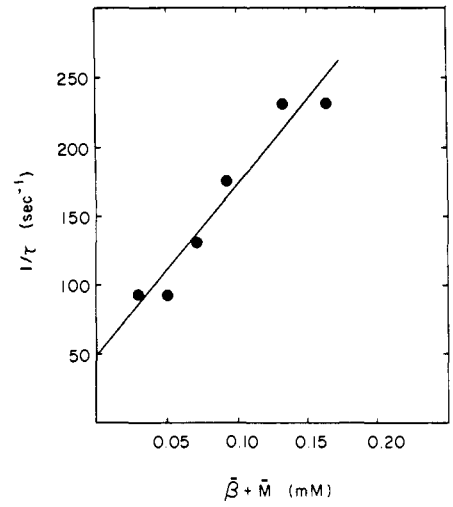

Figure 7. Dependence of $1/\tau$ on $\bar{\beta} + \bar{M}$. These values of $\bar{\beta} + \bar{M}$ were determined from the experimental values of $[\beta^{PMB}]^0$ and $[MIN]^0$ using $K_D = 4 \times 10^{-5}$ M.

Table I. Relaxation Times for Interaction of Methylisonitrile with Hemoglobin β Chains[a]

Sample	β^0, mM	M°, mM	$\bar{\beta} + \bar{M}$, mM[b]	$\bar{\beta} + \bar{M}$, mM[b]	$K_D \times 10^5$, M[b]	$1/\tau$, sec^{-1}
1	0.017	0.02	0.025	0.032	2.3	92
2	0.038	0.04	0.050	0.050	4.3	93
3	0.06	0.07	0.08	0.07	5.3	130
4	0.097	0.10	0.105	0.091	5.9	175
5	0.144	0.18	0.124	0.132	3.5	231
6	0.21	0.25	0.148	0.163	3.2	229

[a] pH 7; 0.2 M phosphate buffer; initial temperature = 20°, final temperature = 26°. [b] Determined optically. [c] Determined from T jump fit value of $K_D = 4.0 \times 10^{-5}$ M.

k_1 (and therefore $K_D = k_{-1}/k_1$). Using the value of K_D obtained, new values for $\bar{\beta} + \bar{M}$ were calculated from the more accurately known initial concentrations of β^{PMB} and MIN and plotted vs. $1/\tau$. The resulting values for the rate constants obtained from this iteration were $k_{-1} = 49$ sec^{-1}, $k_1 = 1.24 \times 10^6$ M^{-1} sec^{-1} (see Figure 7). The resulting $K_D = 3.9 \times 10^{-5}$ M is both in agreement with the literature value ($K_D = 3.1 \times 10^{-5}$ [23]) and about equal to the average of the values calculated from the optical spectra ($K_D = 4.1 \times 10^{-5}$, see Table I).

Discussion

The agreement between the calculated average temperature rise and the observed temperature rise is very good; cf. 6.7° vs. 7.2° for the set-up shown in Figure 1B, 5.7° vs. 6.0° with optical flat added, 13.9° vs. 13.4° for filter removed, and 4.1° vs. 5.1° for filter removed and charging voltage reduced from 2.4 to 1.7 kV. This agreement indicates that the computer simulation gives a valid representation of the multipass laser apparatus. Given that the observed temperature rises, while large and more than sufficient for temperature jump relaxation experiments, are much less than the maximum temperature rise (136°) if *all* of the energy from the laser were absorbed by the water sample, the computer simulation can then be used to determine where the energy losses occur with the present set-up. A priori, the possible causes of loss of laser energy are (1) divergence of the beam, (2) losses from components within the cavity (especially the uncoated components), and (3) the fact that the cross-sectional area of the cell is less than that of the beam. The simulation shows that the number of complete circuits through the cavity before the energy is reduced to 1% is only of the order of 5. By that stage the beam has been attenuated by the combination of losses on all of the surfaces, especially the filter, and by failure to pass through the cell in particular. The aperture restrictions are sufficiently severe that the nonsquare cross-sectional energy profile of the laser beam is insignificant. While the losses reduce the overall temperature rise they improve the homogeneity of the heating of the cell as can be seen from the heating profile obtained without the filter. Since more passes can be sustained along the axis of the cell, the heating profile is more dome shaped.

Despite the fact that *all* of the laser energy cannot be effectively utilized with the present design, the temperature rise obtained is *large and homogeneous*, the construction is simple, the operation is stable, and no dyes need be added to the solution. In addition, there is a high potential for very large temperature rises (20–100°) by having the sample within the laser cavity. Simple alternative cavity configurations using concave mirrors rather than lenses are possible,[20] which greatly reduce the losses due to either divergence of the beam or components other than the sample itself within the cavity. Also the intracavity configuration does not preclude Q switching the laser to simultaneously achieve very rapid heating times (~10–100 nsec) and homogeneous heating. This subject is presently under investigation.

The equilibrium constant obtained for the interaction of hemoglobin β chains with MIN is in agreement with the literature value,[23] and the rate constant k_{-1} is the same as that determined for this reaction under similar conditions ($k_{-1} = 57$ sec^{-1} at 20°) using nuclear magnetic resonance methods (except that the NMR experiment was in D_2O[19]). No evidence was obtained that the reaction is not a simple bimolecular binding, but the plot of $1/\tau$ vs. $\bar{\beta} + \bar{M}$ could not be carried to higher concentrations because of precipitation of the β^{PMB} chains. The NMR results were also analyzed as a simple bimolecular reaction.

The stability of this particular biological system to laser temperature jumps is demonstrated by the fact that there was no change in successive temperature jump transients. This system is expected to be a relatively sensitive test of photodegradation since it is a protein subunit containing an absorbing prosthetic group and an oxidizable metal.

Conclusion

By placing the sample cell within the laser cavity, large homogeneous laser temperature jumps can be obtained. The system is particularly simple and stable, and the potential

for larger temperature rises (20–100°) with simple alternative configurations is great.

Acknowledgment. The financial support of the National Institutes of Health (Grant GM-17190 (B.D.S.) and Training Grant Fellowship (J.H.B.)) and the Alfred P. Sloan Foundation (Fellowship to B.D.S.) is gratefully acknowledged.

References and Notes

(1) Department of Chemistry.
(2) Division of Engineering and Applied Physics.
(3) Address correspondence to this author.
(4) E. M. Eyring and B. C. Bennion, *Annu. Rev. Phys. Chem.*, **19**, 129 (1968).
(5) E. M. Eyring, Final Technical Report, AFOSR, Grant AF-AFOSR-476-66-A, December 1967.
(6) J. V. Beitz, G. W. Flynn, D. H. Turner, and N. Sutin, *J. Am. Chem. Soc.*, **92**, 4130 (1970).
(7) E. F. Caldin, J. E. Crooks, and B. H. Robinson, *J. Phys. E.*, **4**, 165 (1971).
(8) H. Hoffman, E. Yeager, and J. Stuehr, *Rev. Sci. Instrum.*, **39**, 649 (1968).
(9) K. J. Ivin, R. Jamison, and J. J. McGarvey, *J. Am. Chem. Soc.*, **94**, 1763 (1972).
(10) N. Sutin and C. Creutz, *J. Am. Chem. Soc.*, **95**, 7177 (1973).
(11) J. K. Beattie, N. Sutin, D. H. Turner, and G. W. Flynn, *J. Am. Chem. Soc.*, **95**, 2052 (1973).
(12) D. H. Turner, G. W. Flynn, N. Sutin, and J. V. Beitz, *J. Am. Chem. Soc.*, **94**, 1554 (1972).
(13) E. F. Caldin, M. W. Grant, B. B. Hasinoff, and P. A. Tregloan, *J. Phys. E.*, **6**, 349 (1973).
(14) E. F. Caldin, M. W. Grant, and B. B. Hasinoff, *J. Chem. Soc. D*, 1351 (1971).
(15) E. F. Caldin, M. W. Grant, and B. B. Hasinoff, *J. Chem. Soc., Faraday Trans. 1*, **68**, 2247 (1972).
(16) J. E. Crooks and B. H. Robinson, *Trans. Faraday Soc.*, **66**, 1436 (1970).
(17) M. W. Grant, *J. Chem. Soc., Faraday Trans. 1*, **69**, 560 (197).
(18) H. Staerk and G. Czerlinski, *Nature (London)*, **205**, 63 (1965).
(19) B. A. Manuck, J. G. Maloney, and B. D. Sykes, *J. Mol. Biol.*, **81**, 199 (1973).
(20) J. H. Baldo, Thesis, Harvard University, 1974.
(21) The rate output of the laser provides a valid estimate of the intracavity energy density since the laser is normally operated with a low reflectivity (~8%) front mirror.
(22) H. Gutfreund, "Enzymes: Physical Principles," Wiley-Interscience, London, 1972.
(23) B. Talbot, M. Brunori, E. Antonini, and J. Wyman, *J. Mol. Biol.*, **58**, 261 (1971).

Triplet State Electron Paramagnetic Resonance Studies of Zinc Porphyrins and Zinc-Substituted Hemoglobins and Myoglobins

Brian M. Hoffman

Contribution from the Department of Chemistry, Northwestern University, Evanston, Illinois 60201. *Received August 19, 1974*

Abstract: Electron paramagnetic resonance studies of photoexcited, five-coordinate zinc mesoporphyrin IX (ZnMesoPor) and protoporphyrin IX (ZnPor) complexes have demonstrated the importance of vinyl-group conjugation and axial-ligand π bonding in determining the properties of the lowest metalloporphyrin triplet state. The conformational properties of that state have also been discussed. In addition, ZnPor and ZnMesoPor have been incorporated into the heme crevice of apohemoglobin and apomyoglobin, and the triplet state properties of these zinc-substituted hemoproteins have been studied. Differences between the porphyrin–protein interaction in T-state hemoglobin and myoglobin (an analog for R-state hemoglobin), and chain differences within the T state, are observed and discussed.

Zinc porphyrins are diamagnetic in their ground state, with a tendency to bind a single additional ligand to the zinc atom.[1] The lowest lying porphyrin triplet state is sensitive to perturbations of the zinc porphin core and in this work electron paramagnetic resonance (epr) studies of photoexcited, five-coordinate zinc mesoporphyrin IX (ZnMesoPor) and protoporphyrin IX (ZnPor) complexes are used to examine the effects of lateral substituents and of coordinating nitrogenous bases to the metal. In addition, ZnPor and ZnMesoPor have been incorporated into the heme crevice of apohemoglobin and apomyoglobin, and the triplet state properties of these zinc-substituted hemoproteins have been studied. The influences of the protein environments of myoglobins (Mb) and hemoglobins (Hb) are compared, the 1-methylimidazole complexes of the zinc porphyrin–dimethyl esters serving as reference model compounds.

Porphyrin Triplet State

Closed-shell metalloporphyrins exhibit a metastable photoexcited triplet state which can be studied by epr.[2,3] In the "four-orbital" model of porphyrin excited states, the lowest triplet state of a fourfold symmetric porphyrin is largely independent of the metal atom and is spatially doubly-degenerate (^3E_u). An excited "square" porphin skeleton is Jahn-Teller unstable and is subject to a symmetry-breaking distortion into two equivalent, $S = 1$, vibronic states. These states may interconvert and, in the absence of further effects, are still of equal energy, but the orbital angular momentum and spin–orbit coupling expected of an ^3E state are quenched. Interactions with substituents on the porphin core, with axial ligands, as well as nonbonded interactions with the environment can lift the vibronic degeneracy and selectively stabilize one vibronic state by an energy, δ.[4,5]

The epr transitions of a triplet-state molecule can generally be described by the spin Hamiltonian: $H = g\beta\mathbf{S}\cdot\mathbf{H} + DS_z^2 + E(S_x^2 - S_y^2)$. Considering the zero-field splitting (ZFS) parameters, D is a measure of the spatial distribution of the triplet-state wave function, $D \propto \langle(3z^2 - r^2)/r^5\rangle$; E is a measure of the tetragonal distortion, $E \propto \langle x^2 - y^2\rangle$.[6] If symmetry-breaking perturbations split the vibronic states of the photoexcited ^3E level by an energy $\delta \gg kT$, the porphyrin undergoes a static distortion, E is nonzero,[4,5] and adjacent x and y transitions are split by $\delta H_{x,y} = 3E/g_e\beta_e$.[6]

In many of the spectra reported here the nature of the peaks in the region of the x–y transitions is, however, determined by a kind of dynamic Jahn-Teller effect. When kT approaches or exceeds δ, both vibronic states become populated. As the porphyrin interconverts between vibronic